DUCTILE FRACTURE BEHAVIOR OF CAST STRUCTURE CONTAINING VOIDS

Ph. GILLES & C. MIGNE, FRAMATOME ANP

Tour Framatome - Cedex 16 – 92084 Paris La Défense - France

S. CHAPULIOT, Commissariat à l'Energie Atomique (CEA)

DRN/DMT/SEMT/LISN, 91191 Gif sur Yvette, France

KEYWORDS: Failure – Mechanisms – Simulations.

Introduction

In Pressurized Water Reactors, the primary loop contains cast-piping components made of duplex stainless steel. Due to the presence of ferrite, such steels are susceptible to thermal aging embrittlement, which decrease their fracture resistance. The cast process induces shrinkage cavities, therefore all these components are submitted to liquid penetrant examination and all surface defects are repaired. The French utility EDF and FRAMATOME have launched an important research program over the last twenty years to assess the resistance of aged cast components [1-3]. For example: accurate correlation have been established between toughness and chemical composition, ferrite content, aging conditions of components and Fracture Mechanics tests have been conducted by EDF on cracked pipes and elbows having a predicted low end-of-life toughness.

More recently, EDF, CEA and FRAMATOME have conducted experimental and analytical analysis of fatigue and fracture behavior of aged cast stainless steel structures containing shrinkage cavities. The present study considers only ductile tearing. The objective of this paper is to explain why such structures behave like defect free ones up to loads higher than yield limit load, but if ductile tearing occurs, total failure may follow rapidly. The explanation is based on specimen test results and a Fracture Mechanics model of the interaction between shrinkage cavities.

Experimental studies

Three series of fracture tests have been carried out on specimens containing shrinkage cavities. EDF and CEA have compared the fracture behavior of SENT type specimens with cast defects instead of a crack and parent SENT with an envelope crack of the defects. In these two series of experiments, the number of cast defects per specimen is rather low, which is not representative of groups of numerous small voids observed in components. Our paper focuses on the third series of tests conducted by CEA on large tensile specimens with a high density of cavities.

The complexity of manufacturing mockups with shrinkage cavities and their size limited to four the number of tests. First, a duplex stainless steel rather sensitive to ageing is selected: the percentage of equivalent chromium content Cr* (%Cr + %Si + %Mo =26%) and δ ferrite content estimated from the chemical composition (28%) are high in comparison with values measured on components. Second, a plate is cast from this material with a too small volume of feedheads in order to create a large number of cavities. Then shrinkage cavities are located in the plate from X-ray measurements and the bars are cut in areas containing voids of not too large volume (ranging from 1 to 3 in the ASTM classification). The bars are machined before being thermally aged during 3000 hours at 400°C. Tensile test and fracture test specimen are cut inside the ingot in a free of defect zone, but not too far from the bars.

The total dimensions of the bars are 490-mm length, 110-mm width and 50-mm thickness. In the efficient zone, where defects are located, the section is reduced to 95 mm (90 at the end of test) by 25 mm. In our paper, we consider 2B = 90 and t = 25.

Shrinkage cavities have been identified in the fractured section accounting for coloration due to thermal ageing or higher surface roughness in voids. From enlarged photographic prints, mappings of shrinkage cavities were made for the four specimens (see Fig. 1). The importance of these groups of cavities was measured by summing the length of the voids along lines parallel to the width direction. Histograms of 29 to 31 bars were established for each test. The average value of the cumulated length gives an estimation of the reduction of area X due to the presence of shrinkage cavities. These values are reported below in Table 1.

Test ID	322	323	324	325
Reduction of area %	6,0	12,9	6,2	7,7

Table 1. Reduction of area due to shrinkage cavities

Figure 1. Mapping of shrinkage cavities in the 323 specimen

Tensile characteristics and toughness have been measured at room temperature after ageing (3000 hrs at 400°C). An important scatter is observed on the stress-strain curve. This may be explained by the small size of tensile specimen compared to the grain size. Over the five stress-strain curves, only three should be selected: they are very close to each other and to rationale stress-train curves deduce from the

force-displacement curves measured on the bars. The mean values of the tensile characteristics of these three specimens are given in Table 2.

E (MPa)	$R_{p0,2}$ (Mpa)	R_m (MPa)	S_f (MPa)	Ultimate ε %
197867	357,3	665	511	8,5

Table 2. Mean values of tensile characteristics

The J-R curve has been derived from four CT20 tests using the CFR procedure [4].

$$J = 148{,}09(\Delta a)^{0{,}3652} \qquad (1)$$

Where the ductile crack growth Δa is in mm and J in kJ/m^2. The value of J for 0,2 mm of extension (and for the mean value of flow stress) is 86 kJ/m^2.

The tests were performed at room temperature on a hydraulic press. The two ends of the bars are respectively embedded to the lower and upper parts of the press. A vertical monotonically increasing displacement was applied by a stroke to the bars up to failure. The press force and displacement transducers respectively measure the applied load and displacements. Two strain gauges are stuck on both sides of the bar, at the middle, where defects are located (defect zone strain). Two other gauges measure the remote strain in the reduced section. Two clip gages are fixed symmetrically on both sides of the defect area, giving a mean (remote) strain. The defect extension is measured using a potential drop technique. During the test, small unloadings are applied periodically in order to identify any stiffness reduction.

The four following criteria were proposed for initiation of defect extension:
- Global offset. Local strains should be proportional to the mean strain. But any change of geometry like crack initiation from voids may bend the slope of the regression line: the offset is the difference between instantaneous and predicted measurements. The global offset is given by remote strain-mean strain correlation.
- Local offset is given by defect zone strain versus mean strain correlation.
- Partial unloadings give the elastic slope of local strain versus mean strain.
- Failure of gauges in the defect zone.

The experimental results may be summarized as follows:

A - The force-applied displacement curves are on the top of each other. The same is almost true for the force-mean strain curves, the applied displacement-mean strain curves and the Potential Drop-applied displacement curves. We conclude that defects have a very low influence on the global behavior of the specimens.

B - All the initiation criteria give almost the same results. The partial unloading technique seeming to be the more reliable, only the corresponding results are reported in Table 3. These results are given in term of conventional stress, i.e. the ratio of applied force to nominal section area (90x25).

C - The "initiation" stress is almost independent of the size of the defect: the standard deviation represents only ± 1,2 % of the average value (567,5 MPa).

D - Failure stress values (see Table 3) reveal two types of behavior. For the three specimen 322, 324, 325 the failure stress has the value of Rm (4% less for the 324 bar) and is 14 to 19% higher than the "initiation" stress. For the 323 specimen, the failure stress is 10% lower than Rm and only 4% higher than the "initiation" stress. As shown on Figure 2, these results are clearly correlated to the amount of reduction of area only in the case of a large defect (323 bar)

Test ID	322	323	324	325
"Initiation" stress	568	578	559	565
Failure stress	667	601	636	673
Ratio failure/initiation	1,17	1,04	1,14	1,19

Table 3. Tests results

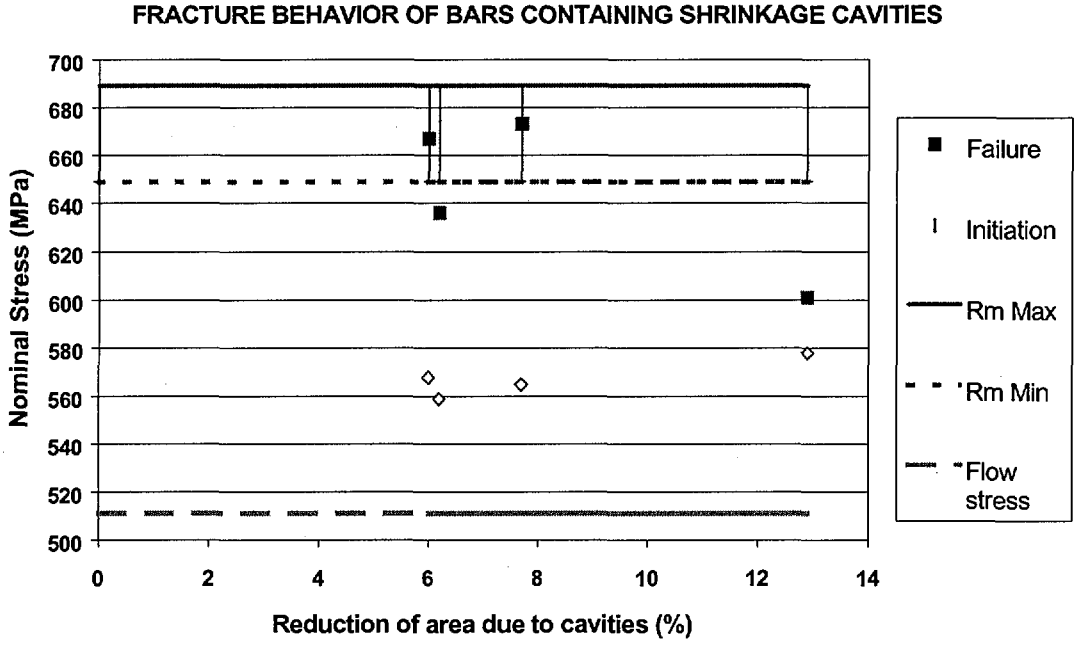

Figure 2. Nominal stress (applied/R_{p02}) results

Further comments on the experimental results

In order to get a better understanding of the failure behavior of the tested bars, more attention has to be paid to what is considered as "initiation" in the tests.
All the values of "initiation" stress are almost identical. This can not correspond to an extension in the width direction for two reasons. First the size of the envelope of voids is almost two times larger in the 323 bar than in the other bars, and force causing defect extension depends on its initial geometry. Second, since it is well known that a few % extension of an embedded defect has little influence on the structural behavior, the change of stiffness evidenced by the partial unloadings should correspond to a break trough the thickness. In the thickness direction the peak density of voids is around 50%, for all the bars, but this trough thickness density varies largely along the width as presented on the following diagrams (Figs. 3a & b).

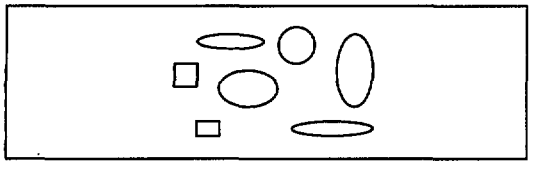

Fig 3a: 323 type of bar

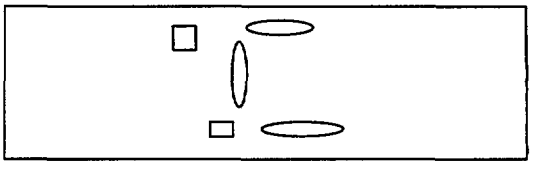

Fig 3b: 322 type of bar

The breakthrough results obviously of ligament failures between voids: the true initiation of cracking begins when a void extents. This phenomenon is the initiation of void coalescence, further mentioned as the local initiation. Test instrumentation failed to indicate local initiation in all four specimens. During the tests, in the defect area the skin became as an orange peel, which is a sign of intense yielding probably due to coalescence of internal voids. This corresponds to the loss of proportionality between local strains measured in the defect zone and remote strains as shown on the following graph (Fig. 4).

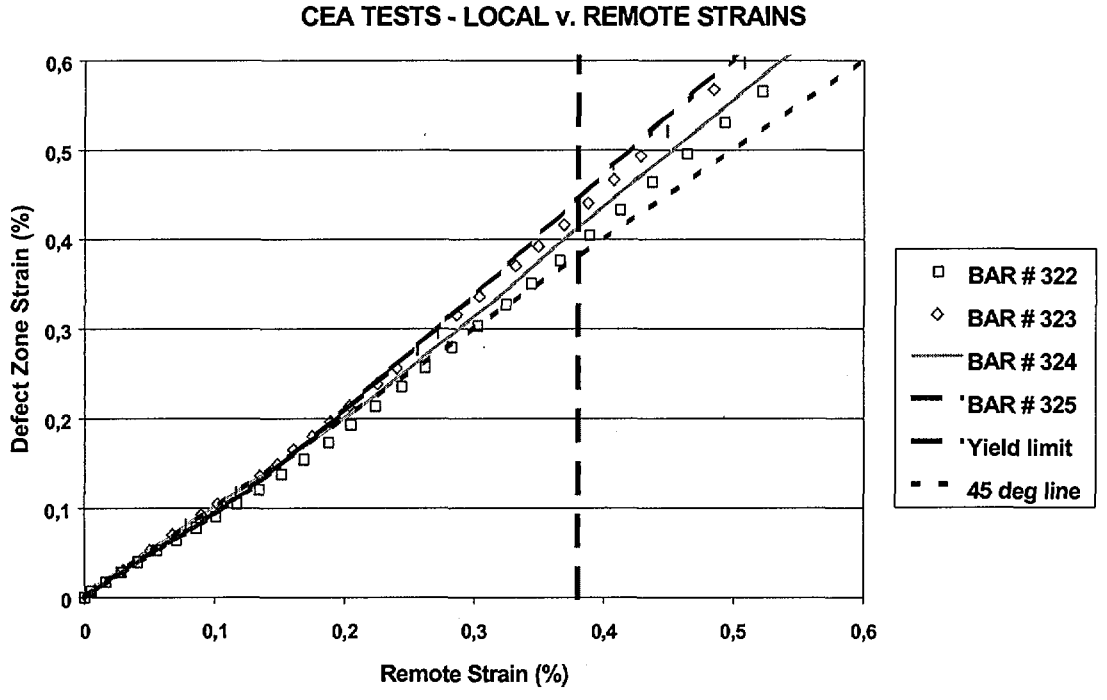

Figure 4. Variation of the trains measured in the defect zone as a function of remote strains.

The departure from linearity appears clearly below the yield stress (357 MPa), far below the measured "initiation" (≈ 565 MPa) which is above the flow stress (511 MPa). Measured "initiation" cannot be considered as an (upper bound) estimate of local initiation. We think that it corresponds to the apparition of a trough-wall crack. The four criteria measuring "initiation" give a qualitative indication of stiffness change, which indicates a breakthrough, but do not inform about the length of the trough-wall crack. We will call it the generalized initiation and present below a tentative explanation of the generalized initiation stress invariability with the initial reduction of area.

Void coalescence is driven by the strong stress concentrations, which depend on the void size and its ratio to the ligament between voids or void and free surface. This may be illustrated by the variation of Stress Intensity Factors at the ends of two through-wall coplanar cracks of different length [5].

$$K_1 = \sigma F\left(\frac{a_2}{a_1}, \lambda\right)\sqrt{\pi a_1} \quad (2).$$ Where $\lambda = \frac{a_1 + a_2}{a_1 + a_2 + t}$ and t is the ligament size.

The λ factor varies from 0 when cracks are very far from each other to 1 for connecting cracks. For $a_2 = a_1$, $F = F_{aa}$ [6] varies from 1 to infinity when λ increases from 0 to 1. For unequal cracks, F is larger for the smaller crack than for the larger one, but the size effect is greater than the interaction effect and if $a_2 > a_1$, then $K2 > K_1$. However, crack growth between two interacting cracks does not depend only on the maximum SIF. For analyzing the effect of crack distribution on the coalescence, we compare the evolution of two configurations of coplanar cracks propagating in fatigue. In the first case, the initial crack lengths are respectively 8 and 2 and are distant of 2,5. In the second case, the ligament and the envelope of the cracks and ligament have the same value, but the cracks are equal, their length is the 10/2 = 5.

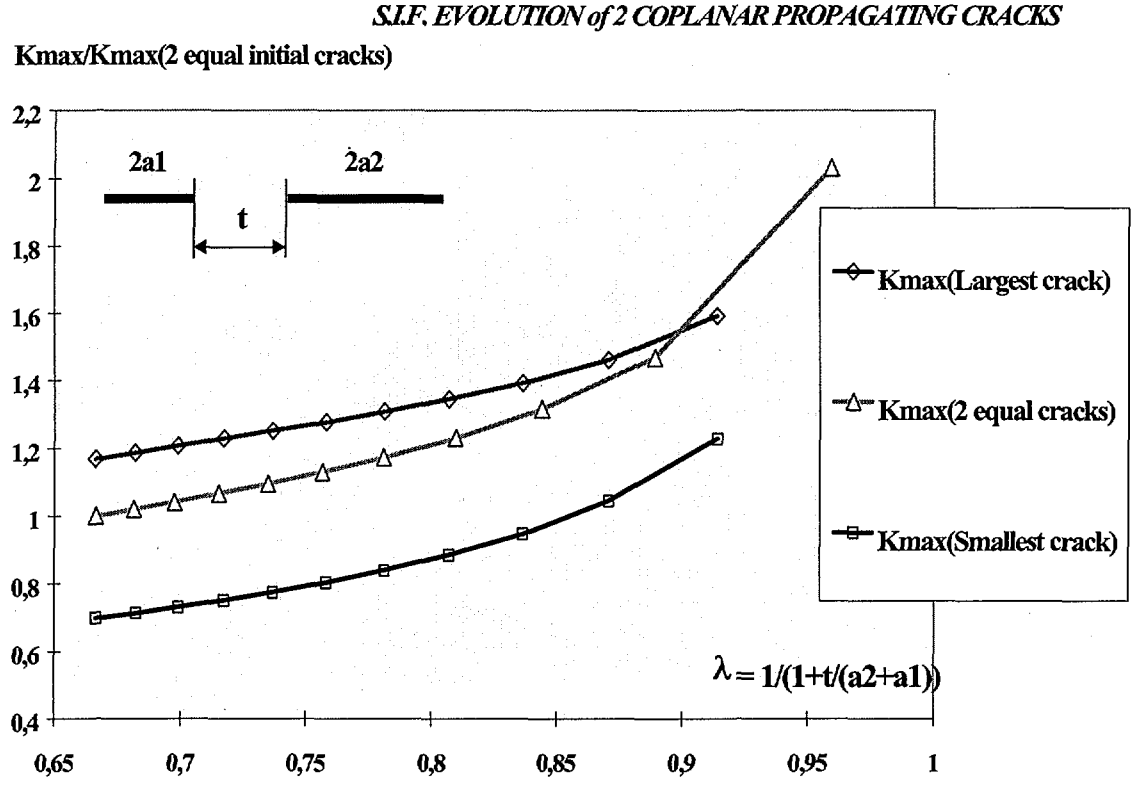

Figure 5. Comparison of growth of 2 coplanar interacting cracks, with a same total initial length, but having either equal or unequal length.

The cracks propagate following a Paris law: $da = C[\Delta K]^m dN$, where N is the number of cycles and C, m are constants depending on the material. In the two configurations, we consider the same material and loading. The crack extension is computed cycle by cycle, assuming the SIF constant during the cycle. This underestimates the growth, but does not make any difference for the purpose of our demonstration. We compare the evolution of SIFs at the interacting tips from which depends the speed of crack tip extension. Figure 5 shows that the SIF for two equal cracks is closer to the large crack SIF than to the small crack SIF and becomes greater than the large crack SIF when the ligament is small compare to the total crack length. Fatigue coalescence is almost independent of relative crack size, but is strongly influenced by the cumulated crack length and ratios of ligament sizes to the sum of sizes of neighboring cracks.

The same should be true for any type of ligament reduction depending strongly on SIF values of like ductile tearing: coalescence depends mainly on the cumulative size of interacting voids. Since peak values of reduction of area in thickness direction are comparable and material characteristics identical in the four specimens, then the applied forces at coalescence should be of same order of magnitude. Considering an embedded crack having the same surface as the sum of void projected area on the section normal to the loading direction could make a prediction of the generalized initiation stress.
Hence, we conclude that at the generalized initiation stress, a trough-wall crack exists over one part of the defect zone. We will check thereafter if failure may be predicted by a stability analysis of a trough-wall crack whose length 2a is an unknown fraction η of the reduction of area times the specimen width ($a = \eta * X * B$). For this purpose, we used a J-estimation scheme for through-wall cracked plates we developed several years ago in the frame our work on schemes for pipes & elbows [7]. This J formula, based on GE-EPRI results, is described briefly in the appendix. The stability analysis is illustrated on Figure 6.

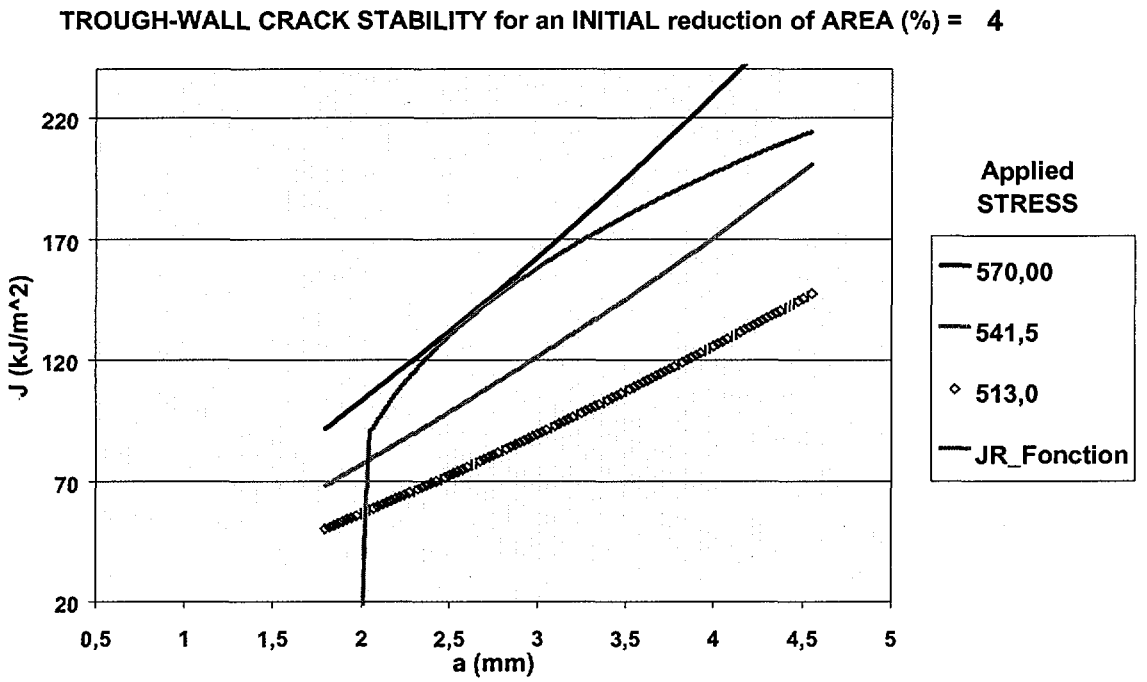

Figure 6. Stability analysis of trough-wall cracked bars of SEMT type.

Considering the measured values of failure stress, i.e. 601 MPa for 323-bar and 667 MPa for 322-bar (which is close to R_m = 665 MPa as for 324 and 325), we obtain the following size for the associated stable trough-wall cracks:

Tested bar	Gen. Initiation	Failure stress	Crack length 2a (mm)	η factor
323	578	601	2,39	0,20
322	568	667	1,02	0,19

Table 4: Estimation of the trough-wall crack length at instability.

From above, the following scenario may be drawn for the fracture behavior of the bars:
- Phase 1: Local initiation of void growth inside the bar, at a stress level may be around the yield limit (357.3 MPa). No sign of this phase has been detected.
- Phase 2: Coalescence of voids inside the bar ended by a break through around the weakest line parallel to the thickness direction. This is the generalized initiation, which corresponds to formation of a macrocrack from a fraction of the initial group of voids. In present experiments, this happens at a stress level (mean value of 565 MPa) above the flow stress (511 MPa). Only the generalized initiation has been registered.
- Phase 3: Stable crack extension of the through-wall crack and failure by crack instability. In any case, the amount of stable crack extension is short since the level of generalized initiation stress is high. If the J-resistance of the material is low and the trough-wall crack sufficiently large, then generalized initiation is immediately followed by failure (almost the case of the 323-bar). If J-resistance of the material is high or the trough-wall crack too short, then failure will occur by collapse: the failure stress equals the maximum tensile stress R_m (665 MPa).

The size of the trough-wall macrocrack appears to represent about 20% of the initial cumulated size of the shrinkage cavities. The initial reduction of area has been measured on the fractured surface. For the present material (low but not very low J-R curve) if the initial reduction of area is below 10%, then failure stress will be close to the R_m value.

A 2D model for a qualitative explanation of the fracture behavior

For the purpose of understanding the failure behavior of structures containing shrinkage cavities, an elementary 2D model was established. The basic idea is that the main difference of fracture behavior between a structure containing a group of voids and the same structure where a unique crack is substituted to the voids, is the existence of a phase of void coalescence in the first case.

Since stress singularities are higher at reentrant corners, shrinkage cavities will extent at these corners at very low level of loading. For describing coalescence between cavities, this regularization of the surface may be neglected. Therefore a fracture mechanics model of a group of shrinkage cavities may be considered based on a combination of cracks and elliptical voids. Interaction of randomly spaced and oriented defects of holes and cracks has been treated by M. Kachanov, but only in the elastic case [8]. Even for a small number of defects, solving the problem requires a computer code and most of the results given by authors are in terms of variations of elastic moduli. Kachanov underlines the inadequacy of modelling a microcraked structure by effective elastic materiel for failure analysis, but do not propose a way to describe nucleation and growth of small defects.

In a structure containing a large group of voids, extension of the envelope of the group (generalized initiation) represents a dangerous event for the structure. This will occur when ligaments are broken, at the end of coalescence. The first break of a ligament is controlled by local initiation, which appears at the void combining large size and highest interaction with its neighbors. Once the first ligament broken, the

new microdefect will interact more with the remaining voids if the void density is still high in this area. We may consider that coalescence is an accelerating process in zones of high density inside the group. Depending on the void distribution, coalescence constitutes of one or several similar steps. We propose to describe a typical step of coalescence by considering an elementary configuration that consists in a plate with two centered cracks and subjected to a uniform tension. As explained before, the crack growth process does not differ strongly if crack lengths are equal or not.

In order to compare ductile tearing behavior of two interacting cracks to their envelope crack, a large number of elastic-plastic calculations need to be performed. This makes a simplified but reasonably accurate model strongly desirable. However, to our knowledge, for multiple cracks elastic-plastic studies are very few (see [9]) and do not provide explicit formulae as in the elastic case. Thus, we developed a model for the present configuration, starting from the one crack model presented in appendix and elastic-plastic finite element computations using computer general code SYSTUS®.

The J formula for two interacting cracks is written as the product of four terms:

$$J_s = J^e \cdot \gamma \cdot \phi^e . \phi^p \qquad (3)$$

Where
- J^e is the elastic value of J for a single crack.
- γ is the yield correction factor for a single crack (=J/J^e).
- Φ^e is the elastic interaction correction factor.
- Φ^p is the plastic interaction correction factor.

We use for J^e the plane strain solution based on the Feddersen-Tada F_t size correction formula [10] in tension: $J^e = \frac{(1-\nu^2)}{E}(\sigma F_t)^2 \pi a$. (4)

The expression of γ is given in the Appendix. We have established a new plastic zone correction Ψ departing from CEGB of GE-EPRI proposals by a more effective attenuating factor. This modification removes the conservatism of the correction (amplified by Φ factors in our case), outside the 0-P_y range.

$$\Psi = \frac{r_y}{a}\exp\left(-\frac{2}{\beta}L_r^{\beta}\right) \text{ with } \frac{r_y}{a} = \frac{1}{6}\left(\frac{\sigma F_t}{\sigma_y}\right)^2 \text{ and } \beta = 0{,}15\exp(6{,}07 . \mu_{ref}) \qquad (5)$$

The elastic interaction correction factor Φ^e comes from the solution of Erdogan [6] for two coplanar equal cracks in an infinite solid under tension: $\Phi^e = [F_{aa}(I_{tip}, \lambda)]^2$ with I_{tip} is the index for the considered crack tip and $\lambda = \frac{2a}{2a+t}$.

We have derived the plastic interaction correction factor Φ^p by analyzing several finite element results obtained for a given stress-strain curve. The solution is based on the fact that yielding must be a function of the ligament size and the load level. We observe that the correction tend to saturate for extended yielding ($L_r \geq L_{rf}$ =1,5). The asymptotic value D is a linear function of t/2a for each tip. The dependence of the Φ^p with the load level is more complex: we have fitted a power law of L_r and λ on the numerical results, but the resulting function is not very sensitive to the parameters.

$$\Phi^p = 1 + D\frac{f(L_r)}{f(L_{rf})} \qquad \text{With } f(L_r) = \left[\frac{\exp(1)\, L_r}{L_{rf}}\right]^{\frac{k}{L_r}} \quad (6)$$

The coefficients D and k are given in Table 5.

Test ID	Asymptotic value D	Slope coefficient k
Tip A	0,87 – 0,69*(t/2a)	4,04 - 4,07*λ
Tip B	0,87 – 0,69*(t/2a)	0,76 - 0,62*λ

Table 5. Coefficients of the plastic interaction factor Φ^p

The finite element computations have made for a Ramberg-Osgood stress-strain curve $\varepsilon = \frac{\sigma}{E}\left[1 + \alpha\left(\frac{\sigma}{\sigma_y}\right)^{(n-1)}\right]$ with E=172000 MPa, σ_y = 163 MPa, α = 1 and n = 6 (7).

Obviously the values of the L_{rf} and of the coefficients of functions D and k should depend on Ramberg-Osgood parameters. Probably L_{rf} varies with α, D with α and n and k with n only, but we may consider that the linearity of their dependence with t/2a and λ is general.

This scheme has been used to compare the ductile tearing behavior of a same panel in tension containing either a single small crack of length 2a, or two symmetrical coplanar cracks 2a distant from t, or their envelope of length 4a + t.

Results of stability analyses of two interacting cracks and their envelope

The structure is 90 mm width, cracks and ligament are 4 mm long. The envelope is therefore 12 mm long. The J-R curve, described by the following power law, has been chosen very low for the purpose of the demonstration:

$$J = 148{,}09(\Delta a)^{0{,}3652} \qquad \text{and } J_{Ic} = 11{,}37 \text{ KJ/m}^2 \quad (8)$$

The tensile curve is described by the Ramberg-Osgood law (7).

As shown on Figure 7, interacting cracks are very unstable. The graphs corresponding to single cracks are similar to the one presented on Figure 6. This is due to the strong increase of J with load at the inner tip A. The two cracks growth rapidly in the ligament, before extending on the envelope sides (tips B). The configuration evolves as illustrated on Figure 8. This phase of coalescence is even shorter if cracks are closer to each other (see Table 6 below). In the two cases, ligament instability is immediately followed by initiation of the envelope. The envelope crack becomes immediately unstable if ligament is large enough to allow a sufficient load increase up to ligament instability. In this case generalized initiation stress is the failure stress of the structure.

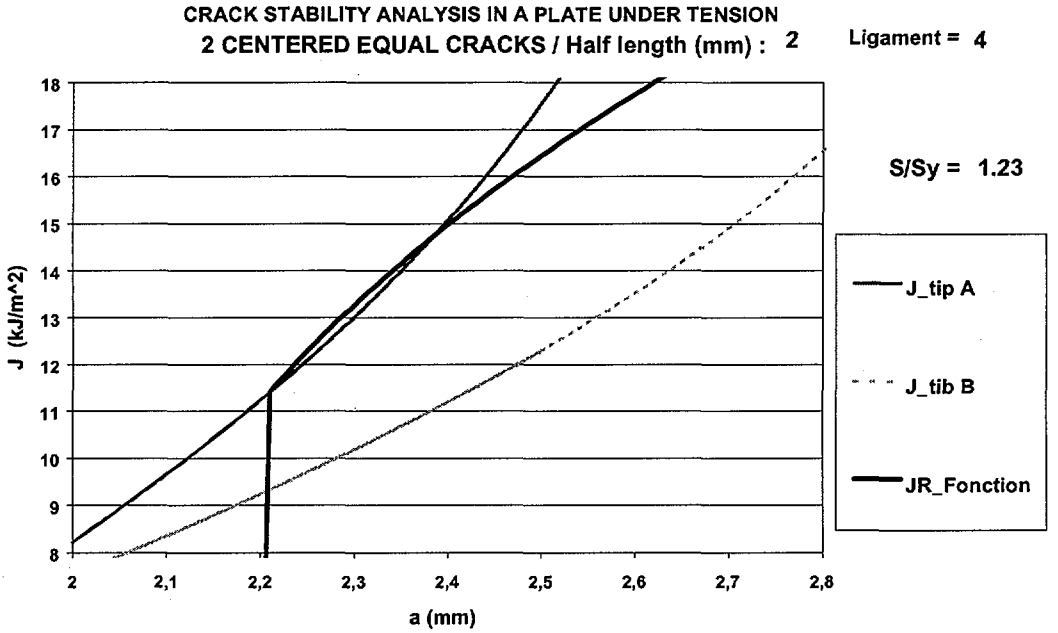

Figure 7. Tearing initiation at the inner tip of two coplanar cracks.

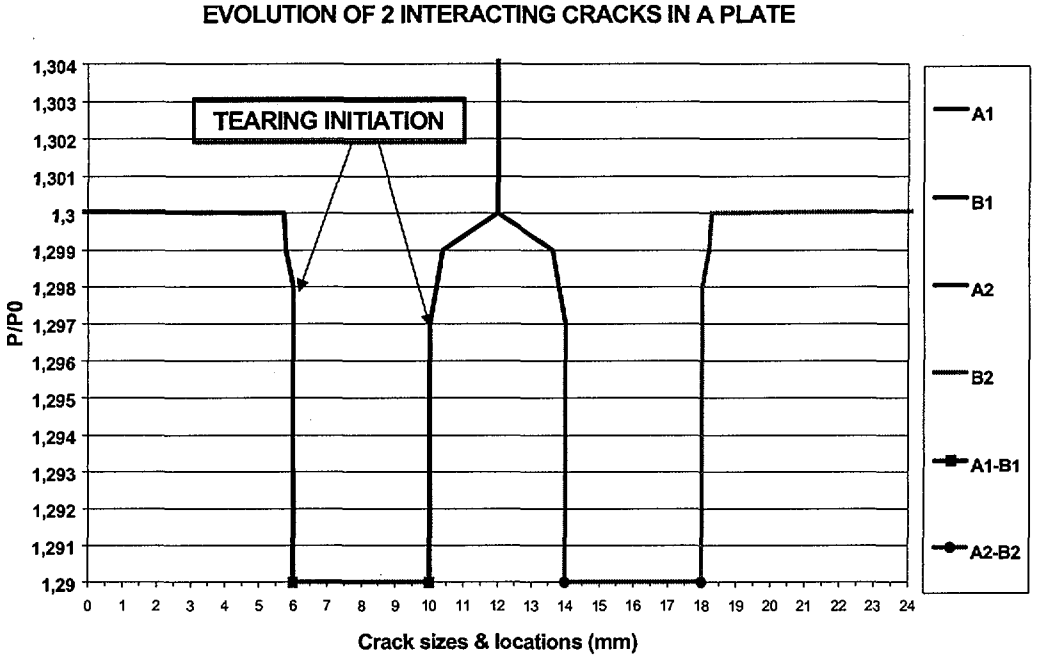

Figure 8. Ductile crack extension of two coplanar cracks.

Configuration	1 crack 2a	2 cracks, t =2a	Envelope 6a	**2 cracks, t =a**	**Envelope 5a**
Initiation	1,33	1,23	1,015	**1,140**	**1,073**
Instability	1,38	1,24	1,085	**1,141**	**1,147**
Ratio	1,04	1,01	1,07	**1**	**1,07**

Table 6: Applied stress/Yield stress ratio at ductile tearing initiation or instability for center cracked panels in tension with a crack 2a, two cracks 2a distant of t and envelope crack 4a + t.

The following conclusions can be drawn from these results:
- Local initiation begins in the ligament.
- Ligament fails before any significant extension on the outer side of the cracks.
- In case of low interaction (initial ligament size equals the crack size: t/2a = 1), local initiation for the group of cracks appears at a stress level much closer to initiation stress of the single crack than initiation stress of the envelope crack. If interaction is high (t/2a < 0,5), local initiation is closer to initiation of the envelope. In case of very high interaction, local initiation may appear at a lower level than for the envelope crack.
- Local initiation is immediately followed by failure of the ligament. In other words, generalized initiation is close to local initiation (see Fig. 7).
- For a low to medium interaction, failure stress of the ligament governs failure of the structure. For medium to high interaction, formation of the envelope is followed by some stable crack extension. But for low J resistant material structural instability follows rapidly generalized initiation.

These conclusions should be valid for unequal cracks, since J is much more sensitive to the ligament/(average of the two neighboring cracks) ratio than to the crack size ratio.

Conclusions

The experimental results presented here show that large groups of shrinkage cavities (representing up to 13% of reduction of area A_r) have almost no influence on the global behavior of the structure. Only for the specimen with the largest reduction of area, a significant reduction of strength has been registered. In this case, the maximum allowable stress is given by the effective stress $Rm^*(1-A_r)$.

Instrumentation (strain gauges, clips, partial unloadings and potential drop) did not produce any information on the damaging process: the measured "initiation" represents the break through the wall of shrinkage cavities. This event should be considered as the formation of a macrocrack and designed as a generalized initiation.

Using elementary fracture mechanics models, it has been evidenced that failure mechanism of structures containing shrinkage cavities consists in 3 phases: local initiation, macrocrack formation by coalescence and failure by crack instability or collapse depending if J resistance is low or not. No significant changes in global behavior appear in the first phase.

Depending on distribution and size of cavities, coalescence has an influence or not on total failure. If the ratio of envelope to cumulated void surface is not too small (> 1,25), and toughness is low, then ligament failure governs total failure of the structure. Thus for such cases, voids will initiate at a higher level than the envelope crack, but this will not be apparent, coalescence will develop rapidly, immediately followed by total failure of the structure. If toughness is high, such structure will fail by global collapse. **We conclude that a group of shrinkage cavities is much less severe than its envelope crack: either material is tough and the structure strength is unaffected by the defect, or the low level of toughness induces tearing around voids, but except if void density is high, this local initiation will appear at a much higher load level than initiation of the envelope.**

Further progress in the comprehension of the physics of the problem could be made in developing an experimental technique to detect local initiation or at least to estimate the size of the break-through. On the other hand, it would be interesting to take advantage from Kachanov's elastic models to develop simplified elastic-plastic fracture mechanics models allowing to perform damage analyses of multi-parameter configurations. The complexity of manufacturing specimens hampers experimental programs on shrinkage cavities, especially for testing representative configurations (large number of small voids embedded in a relatively large specimen in comparison with section area). Unless achieving these two improvements, further experiments will not allow to improve our understanding of the failure mechanisms in structure with shrinkage cavities.

Acknowledgements

The authors greatly acknowledge the colleagues of French utility Electricité De France and CEA that contributed to this program for their fruitful contributions in discussions.

References

[1] G. Bezdikian, H. Churier-Bossennec et al., "Life Evaluation of Cast Duplex Stainless Elbows on PWR Primary Circuit", Proc. 5th Int. Conf. on Nuclear Engineering, ICONE-2490, 1997.

[2] J.-P. Massoud, S. Jayet-Gendrot, et al., "Thermal Ageing of Cast Duplex Stainless Steel Primary Components. Overview of the Research Program conducted by EDF", Proc. 5th Int. Conf. on Nuclear Engineering, ICONE-2497, 1997.

[3] S. Jayet-Gendrot, P. Ould, T. Meylogan, "Fracture Toughness Assessment of In-service Aged Primary Circuit Elbows Using Mini-CT Specimens Taken from Outer Skin", Nuclear Engineering and Design, 184, 3-11, 1998.

[4] Norme AFNOR NF A 03-183.

[5] T. Yokobori, M. Ohashi and M. Ichikawa, "The Interaction of Two Collinear Asymmetrical Elastic Cracks". Reports of the Research Institute for Strength and Fracture of Materials, Tohoku University, Vol. 1. N°2, pp. 33-39.92, 1965.

[6] F. Erdogan "On the Stress Distribution in Plates with Collinear Cuts under Arbitrary Loads". Proc. 4th U.S. Nat. Congr. Appl. Mech., pp. 547-553, 1962.

[7] Ph. Gilles, "J Estimation Scheme For Surface Cracked Pipings Under Complex Loading: Part I & II". Proc. of ECF 11 conference, Poitiers, 1996

[8] M. Kachanov, "Elastic Solids with Many Cracks and Related Problems". Advances in applied mechanics, Vol. 30., 1994.

[9] S. Meyer, E. Diegele, A. Brückner-Foit and A. Möslang, "Crack Interaction Modelling", Fatigue Fract. Engng Mater. Struc 23, 315-333, 2000.

[10] H. TADA, P. PARIS, G. IRWIN, "The Stress Analysis of Cracks Handbook", Del Research Corporation, Hellertown, Pa, USA, 1973

APPENDIX
J-ESTIMATION SCHEME FOR CCT SPECIMENS

The present J estimation scheme is a special case of the J_s, analytical method jointly developed by CEA, EDF and Framatome [A1]. This method is based on the reference stress approach where J is expressed as a product of the elastic solution J^e by a yield function γ, which has the same expression than in the R6 Option 2 approach [A2]. In the present case we selected the CLC option of the J_s method and J^e is given by an explicit formula.

$$J_s = J^e \cdot \left[\frac{E \cdot \varepsilon_{ref}}{\sigma_{ref}} + \Psi \right] \qquad (A1)$$

Where ε_{ref} is the strain corresponding to the stress σ_{ref} on true stress-strain curve of the material and Ψ is the plastic zone correction.

$$\sigma_{ref} = \frac{P}{P_{yref}} \cdot \sigma_y \qquad (A2)$$

The main basic difference between R6 Option 2 and CLC option of J_s consists in the definition of the reference load considered here to differ from the plastic yield load P_{yc} of the flawed structure. The reference load expression takes the following form:

$$P_{ref} = \mu_{Ph}\ \mu_{Pc}\ P_{yPnc} \qquad (A3)$$

The reference load is the product of P_{yc} by a strain hardening dependent coefficient derived in most of the cases from numerical elastic-plastic computations on the cracked structure.

For CCT specimens, we obtained from the GE-EPRI results [A3] the formula (A4) given below. We checked our formulation by comparing predictions with results obtained by the computer general codes SYSTUS®.

$$\boxed{\mu_{Ph} = (1 - \frac{a}{w}) \left[1 + 0.12 \frac{a}{w} + \frac{1}{n} \left(1.41 \frac{a}{w} - 0.83 \right) \right]}$$

References

[A1] M-H. Papin, B. Michel, P. Cambefort and Ph. Gilles, "J Evaluation by Simplified Method for Cracked Pipes under Mechanical Loading", To appear in Proc. 9th Int. Conf. on Nuclear Engineering, 2001.

[A2] Ainsworth, R. A., Engineering Fracture Mechanics, 19 (1984), 633-642.

[A3] V. Kumar, EPRI NP 1931 report, EPRI, Palo Alto, Ca USA, July 1981.